Interfacial activity of graft copolymers in blends: effect of homopolymer molecular weight

P. Sakellariou*
ICI, Paints Division, Research, Wexham Road, Slough SL5 2DS, UK

and G. C. Eastmond
Chemistry Department, Donnan Laboratories, Liverpool University, Liverpool L69 3BX, UK

and I. S. Miles
ICI, Advanced Materials Centre, Wilton TS6 8JE, UK
(Received 23 November 1991; revised 27 January 1992; accepted 18 February 1992)

The effect of varying the homopolymer molecular weight, corresponding to the minor phase, on the interfacial activity of graft copolymers in blends of homopolymers has been investigated. The system studied was polycarbonate/poly(methyl methacrylate) (PMMA) (65/35 w/w) blends containing polycarbonate/PMMA graft copolymers. The molecular weight of the polycarbonate homopolymer was increased from 3.6 to 52.4 kg mol^{-1}, always maintained lower than that of the polycarbonate block (143.8 kg mol^{-1}). Molecular weights of all other components were kept constant. Copolymer interfacial activity, in terms of its efficacy to reduce the size of the dispersed phase and create interface, deteriorated considerably with increasing polycarbonate homopolymer molecular weight. The interfacial area occupied by a single copolymer molecule did not change dramatically. This behaviour was observed with constant (10% w/w) and varying (1–40% w/w) copolymer content. In dilute solutions (1×10^{-3} g cm^{-3}) with selective solvents (toluene), the copolymer formed micelles consisting of approximately nine copolymer molecules with no evidence for significant swelling of the polycarbonate core by unreacted polycarbonate homopolymer. Thermodynamic parameters of aggregation showed the process to be enthalpy driven. Copolymer interfacial activity is discussed in terms of phase diagrams for these systems with increasing homopolymer molecular weight. Phase separation of copolymer and polycarbonate homopolymer from the PMMA-rich matrix as the system crosses the binodal has been argued to be the mechanism to account for the presence of stable fine polycarbonate-rich dispersions in a PMMA-rich matrix. The relative molecular weight of the polycarbonate homopolymer to that of the polycarbonate block controls the position of the critical copolymer–homopolymer concentration relative to that of the overall system.

(Keywords: blends; phase diagram; interfaces; morphology; interfacial activity; copolymer; interfacial concentration; compatibilizer; micelles; polycarbonate; poly(methyl methacrylate))

INTRODUCTION

Modification of heterogeneous polymer blends by adding small amounts of graft or block copolymers is a topic of major practical significance. Copolymer molecules are believed to locate at the interface, create new interface and produce finer dispersion of the minor component. This interfacial activity leads to pronounced changes in the properties of the materials. Provided that the properties of the two phases are carefully mismatched and the interfaces are strong, materials with new properties can be achieved.

It is no surprise then, that a considerable amount of work has focused on the effect of copolymer on the properties, morphology and compatibility of blends[1]. The interfacial tension between immiscible solutions of polymers has been shown to decrease dramatically with the addition of 1–2% w/w of block copolymer[2,3]. Most efficient emulsification of blends has been reported to require the length of the chains in the copolymer to be significantly greater than that of the corresponding homopolymer. Recent theoretical models predict the critical micelle concentration (*CMC*), phase diagrams and interfacial density profiles for monodisperse systems containing block copolymers[4–6].

Despite the large number of publications on specific systems and theoretical calculations, there has been a surprising absence of a systematic study of the molecular parameters influencing the interfacial activity of copolymers in blends. In the most general case of a system consisting of two homopolymers A and B with an added block or graft copolymer CD, the parameters identified either theoretically or from experimental work include:

$$\chi_{AB}, \chi_{AC}, \chi_{CD}, \chi_{BD}, \chi_{BC}, \chi_{AD}$$
$$\Phi_A, \Phi_B, \Phi_{CD}$$
$$M_A, M_B, M_{CD}$$
$$M_A/M_C, M_B/M_C, M_C/M_D$$

* To whom correspondence should be addressed

0032-3861/92/214493-12

where χ, Φ and M denote the polymer–polymer interaction parameter, volume fraction and molecular weight, respectively; the subscripts identify the polymers.

We have already reported on the general effect of the relative molecular weight of the minor component (homopolymer) to that of the copolymer block and copolymer concentration on the interfacial activity of graft copolymers[7,8]. The system studied was a polycarbonate/poly(methyl methacrylate) (PMMA) blend containing polycarbonate/PMMA graft copolymers. This system is a simplified version of the general case where the copolymer blocks are chemically identical to the corresponding homopolymers of the blend (A=C; B=D). We have shown, by varying the polycarbonate block molecular weight, that maximum interfacial activity of the copolymer is achieved when the molecular weight of the polycarbonate copolymer block is significantly greater than that of the polycarbonate homopolymer. In accordance with interfacial tension observations, the copolymer was shown to create significant amounts of interface at concentrations up to ~5 wt%. Thereafter, the interfacial area in the blend did not change markedly. We have argued that at copolymer contents exceeding a critical concentration, location of the copolymer in the bulk phases as isolated chains or micelles is energetically favoured.

This paper reports data on the effect of varying the molecular weight of the polycarbonate homopolymer at constant molecular weight of the corresponding copolymer block. The molecular weight of the homopolymer was maintained smaller than that of the block to ensure efficient copolymer interfacial activity in the blend. The issues addressed in this paper are: the efficiency of the copolymer in creating interface as the molecular weight of the homopolymer corresponding to the minor phase increases towards that of the corresponding block; and the molecular mechanisms responsible for changes in the copolymer interfacial activity in such cases.

The effects of copolymer symmetry (M_C/M_D) and system incompatibility (χ_{AB}) will be dealt with in a separate publication.

EXPERIMENTAL

The PMMA ($\bar{M}_n = 48\,kg\,mol^{-1}$) was obtained from RAPRA Technology Ltd. The polycarbonate (I) was prepared by condensation of an equimolar mixture of bisphenol A and 1,1-bis-(4-hydroxyphenyl)-2,2,2-trichloroethane with phosgene[9].

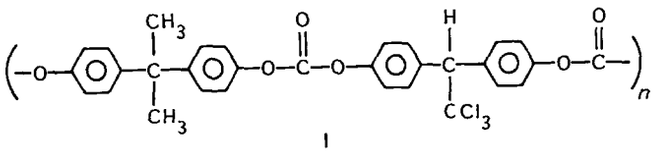

I

The molecular weight of the polycarbonate was dependent on the extent of reaction of the bisphenol and was controlled by careful addition of phosgene in the latter stages of the reaction. Polycarbonates of 3.6–143.8 kg mol^{-1}, with polydispersities typically 2.5, were prepared and carefully purified by several precipitations from toluene into petroleum ether. Molecular weights were determined by g.p.c. with tetrahydrofuran (THF) as the carrier solvent and with a polystyrene calibration.

The polycarbonate/PMMA copolymers were prepared by free radical grafting from the polycarbonate chains (backbone). Photopolymerization[10–12] ($\lambda = 435$ nm) was initiated from radicals formed by abstraction of a chlorine atom from the pendant trichloromethyl groups with the aid of manganese decacarbonyl, $Mn_2(CO)_{10}$. The structure of the reaction product was controlled by carefully adjusting the reaction conditions. Reactions were carried out in dilute solutions (1.5% w/v) of the polycarbonate in methyl methacrylate monomer at room temperature under vacuum and in a room illuminated with inactive sodium light. Radicals were created randomly from only a small percentage of the pendant trichloromethyl groups. Initiation is highly selective and all PMMA chains were attached to polycarbonate backbones. At the low conversions used, no chain transfer to the PMMA occurred. The gelation kinetics of our systems were studied and reaction conditions were adjusted to ensure that kinetics consistent with Flory's gelation theory were obeyed. The relationship between copolymer structure and grafting kinetics have been extensively studied by Bamford *et al.*[13]. The relative crosslinking index (γ_r), is a particularly useful parameter in describing the copolymer structure. It is proportional to the number of crosslinks in the system relative to those necessary for incipient network formation[13]. It was kept at ~0.65. Under these conditions the average structure of the copolymer species[13] can be depicted as:

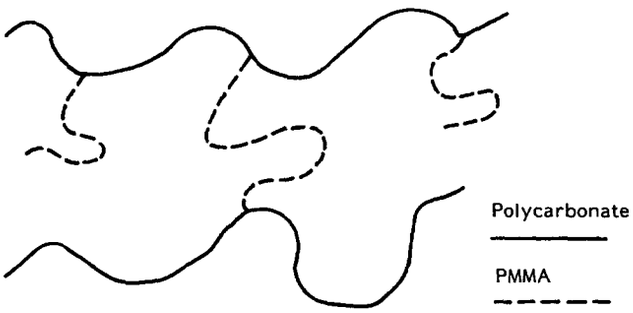

This schematic structure reflects the fraction of PMMA chains terminating by disproportionation (65%) and combination (35%) at room temperature. The composition of the copolymers was determined by means of u.v. adsorption at 230 nm (SP30-UV). Solutions of PMMA and polycarbonate in dichloromethane were separately shown to obey Beer's law at 230 nm with extinction coefficients of 0.64×10^3 and $0.52 \times 10^5\,g^{-1}\,cm^2$, respectively. The significant difference between these two coefficients affords accurate determination of system composition. The weight fraction of polycarbonate was calculated assuming linear additivity of the absorbance of the two components. The molecular weight of the PMMA grafts was determined by selective degradation of the polycarbonate chains by means of a heterogeneous process suggested by Eastmond and Harvey[14]. Molecular weights of PMMA grafts were maintained high in order to ensure efficient stabilization against coalescence of the polymer dispersions during film formation. Molecular weights of the PMMA homopolymer and grafts were determined by g.p.c. with THF as the carrier solvent using a PMMA calibration.

The following abbreviations have been adopted throughout this paper: MAH, $\bar{M}_n$ of polycarbonate homopolymer; MAC, $\bar{M}_n$ of polycarbonate backbone (block); MBH, $\bar{M}_n$ of PMMA homopolymer; MBC, $\bar{M}_n$ of PMMA grafts.

Techniques

Blends were prepared by casting from dilute solutions (4% w/v) in dichloromethane under reproducible conditions. Residual solvent was removed at 115°C under vacuum for over 1 week.

Optical and transmission electron microscopy

Morphologies of the blends were studied by optical and transmission electron microscopy (TEM). Sections (10–15 μm thick) cut normal to the surface of the bulk film (thickness = 200 μm) were used for optical microscopy. Phase contrast arose from birefringence introduced by microtoming. Under these conditions the polycarbonate-rich phases appeared bright and the PMMA-rich phases were dark. TEM was performed on ultrathin sections (80–100 nm) cut parallel to the film surface. Contrast was enhanced by staining the microtomed sections with ruthenium tetroxide vapour. Polycarbonate was selectively stained and appeared dark in the TEM micrographs.

The formation of micelles of the copolymer species in toluene was also studied by means of TEM following the procedure suggested by Price and co-workers[15–18]. A drop of dilute polymer solution ($c = 10^{-3}$–10^{-2} g cm^{-3}) was spread on a carbon-coated TEM grid and the solvent was evaporated under high vacuum (pressure $< 1.33 \times 10^{-4}$ Pa). The polycarbonate chains were stained by exposing the polymer solution to vapour from aqueous ruthenium tetroxide for 30 min.

Membrane osmometry

The *CMC* of the copolymers in toluene was studied by means of Hewlett-Packard high speed membrane osmometers (Models 1 and 2) operating at 310 and 321 K.

Phase diagrams

Phase diagrams of the systems were determined by allowing heterogeneous mixtures of known composition in a common solvent, to separate into two layers and reach equilibrium in tightly sealed glass tubes in a thermostat at 28°C. The internal diameter of the tubes was determined by calibration with distilled water. Phase volumes were determined accurately with the aid of a cathetometer. Total polymer contents of the phases were determined gravimetrically after careful precipitation of a known volume of each phase into petroleum spirits. The relative contents of the two polymers in each phase were determined by ^{13}C n.m.r. spectroscopy from the area under the characteristic resonance due to protons of the disubstituted phenyl in the polycarbonate chain and those of the ester group in PMMA. The samples were dissolved in deuterated chloroform to form 5–8% w/w solutions. In all calculations it was assumed that there was no volume change on mixing. Densities of polycarbonate and PMMA were taken to be 1.30 and 1.20 g cm^{-3}, respectively.

Dynamic mechanical spectroscopy

Dynamic mechanical spectra were obtained using a Rheovibron viscoelastometer (DDV-IIC, Toyo-Baldwin Ltd, Tokyo) on samples (2×30 mm) cut from the cast films. Measurements were made at a heating rate of 10°C min^{-1} and a frequency of 110 Hz with the samples in a nitrogen atmosphere. The instrument was interfaced to a Research Machines microcomputer for automatic data acquisition and reduction.

RESULTS AND DISCUSSION

Two separate experiments were performed to investigate the influence of molecular weight of polycarbonate homopolymer on the interfacial activity of the copolymers in the blends. In all cases the overall blend composition was maintained constant at 65/35 w/w polycarbonate/PMMA. The PMMA-rich phase is, therefore, in all cases the matrix while the polycarbonate-rich phase constitutes the minor (dispersed) phase. The molecular weight of the polycarbonate homopolymer was kept consistently smaller than that of the polycarbonate copolymer backbone. All samples appeared 'homogeneous' or 'nearly homogeneous' under the optical microscope.

Experiment I. Behaviour at constant copolymer concentration

In this experiment, the copolymer concentration was kept constant at 10% w/w. The molecular weight of the polycarbonate homopolymer was increased from ~3 to ~60 kg mol^{-1}. *Table 1* gives the molecular weights of the components used in each system.

The electron micrographs in *Figure 1* show a rapid increase in the average diameter of the polycarbonate-rich dispersions with increasing molecular weight of the polycarbonate homopolymer in the blend (*Figure 2*); all systems consisted of polydisperse polycarbonate-rich dispersions in PMMA-rich matrices. There is no reason *per se* for the systems to give rise to a monodisperse population of polycarbonate-rich domains, as in the case of microphase-separated pure monodisperse block copolymers. The morphology is, therefore, better described by the distributions of domain diameters of the polycarbonate-rich phases (*Figure 3*). At the same time, the amount of interface (*Figure 4*) created by the copolymer decreased with increasing molecular weight of the polycarbonate homopolymer.

The average amount of interface per unit total volume ($\langle S_V \rangle$) and per unit volume of dispersed phase ($\langle S_D \rangle$) were calculated using standard stereological equations[8]:

$$\langle S_V \rangle = 2\mathbf{NL} \quad (1)$$

$$\langle S_D \rangle = 2\mathbf{NL}(\mathbf{LL}/\mathbf{DD}) \quad (2)$$

where **NL** is the ratio of the number of intersections made by a set of at least 10 sampling lines with the boundaries of the dispersions to the total length of the sampling lines, **LL**, and **DD** is the length of the sampling lines traversing the polycarbonate-rich domains. These equations are independent of the system geometry.

It must be noted that phase contrast deteriorated considerably for the system with the shortest polycarbonate homopolymer chains (3.6 kg mol^{-1}).

Table 1 Molecular weight of components for the systems used in experiments I and II

System	*MAH* (kg mol^{-1})	*MBC* (kg mol^{-1})
A1	3.6	248
A2	20.2	248
A3	44.0	248
A4	59.2	248
B1	20.2	389
B2	72.4	389

In all cases *MBH* and *MAC* were 48 and 143.8 kg mol^{-1}, respectively

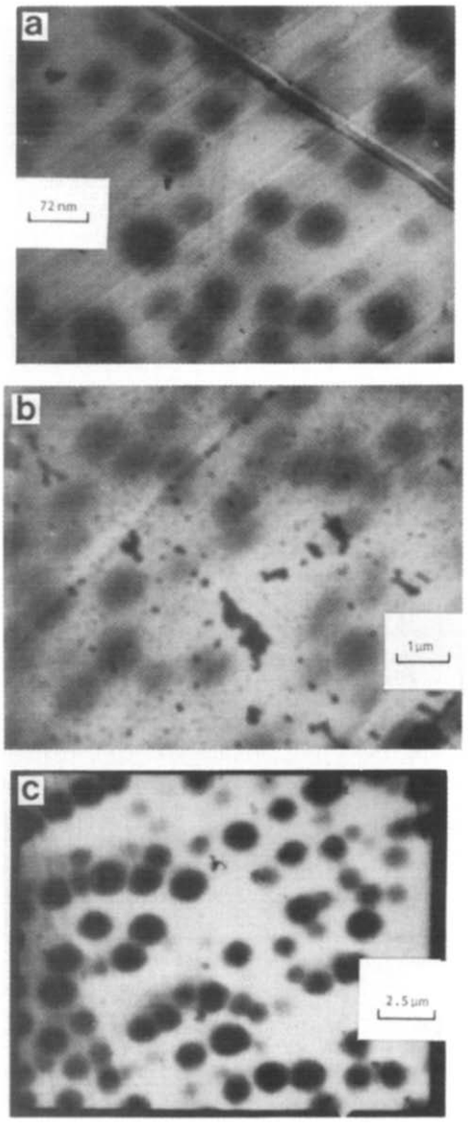

Figure 1 TEM micrographs of the systems in experiment I with increasing molecular weight of the polycarbonate homopolymer (see *Table 1*): (a) A2; (b) A3; (c) A4

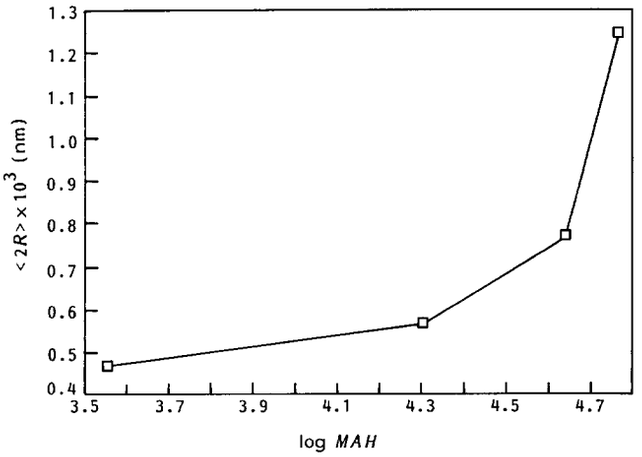

Figure 2 Variation of the average diameter of the polycarbonate-rich dispersions with log *MAH*

Figure 5 illustrates the dynamic mechanical spectra at 110 Hz for the same systems. In agreement with earlier observations[8], a single relaxation was observed for all systems despite the confirmed presence of two phases. The position of the $\tan\delta_{max}$ peak did not change significantly as the polycarbonate relative molecular weight, *MAH/MAC* [where *MAH* is the $\bar{M}_n$ of polycarbonate homopolymer and *MAC* is the $\bar{M}_n$ of the polycarbonate backbone (block)], increased from 0.14 to 1.00 (see *Table 2*). The glass transition temperature, (T_g), taken as the temperature for $\tan\delta_{max}$, corresponds to phases with 62–74% w/w PMMA as calculated with the Fox equation (*Table 2*). This is not far from the bulk composition of these systems at 65% w/w PMMA. As the molecular weight of the polycarbonate homopolymer approached that of the corresponding block the breadth of the relaxation peak broadened noticeably. The system with the shortest polycarbonate homopolymer chain ($MAH/MAC = 0.07$) was too brittle to be tested on the Rheovibron. This behaviour is consistent with earlier observations on similar systems[7,8]. No other relaxation exists at higher temperatures[8]. We have argued that the recorded peak is a composite one, consisting of a relaxation due to the PMMA-rich phase and another one, at slightly higher temperatures, due to the polycarbonate-rich phase. The broadening of the relaxation at $MAH/MAC = 1$ corresponds to changes in the phases in the blends. As the molecular weight of the polycarbonate homopolymer becomes comparable to that of the copolymer block, its solubility into the copolymer-stabilized domains decreases. The increasingly rejected polycarbonate forms a separate phase within the PMMA-rich matrix. This will be expected to be richer in polycarbonate because of increased incompatibility of the two homopolymers. This phase will give rise to a separate relaxation at slightly higher temperatures responsible for the broadening of the composite $\tan\delta$ peak.

Experiment II. Behaviour at varying copolymer concentration

In this experiment, the interfacial activity of two copolymers was studied over a wide range of copolymer concentration, from 1 to 40% w/w. Again the molecular weight of the polycarbonate homopolymer was kept below that of the corresponding copolymer block (see *Table 1*) and the systems appeared 'homogeneous' or 'nearly homogeneous' under the optical microscope.

Figures 6 and *7* illustrate the changes in the morphology of system B2 with increasing concentration of added copolymer. Distribution of sizes of the polycarbonate-rich dispersions generated for the different amounts of added copolymer are illustrated in *Figure 8*. The changes in morphology of system B1 with increasing copolymer concentration has already been discussed elsewhere[8]. Differences between the interfacial activities of the two systems are clearly illustrated in *Figure 9*. The overall behaviour for both systems follows the same

Table 2 Dynamic mechanical data for systems A1, A2, A3 and A4 (see *Table 1*)

MAH/MAC	T_g (°C)	PMMA (w/w %)
1.00	163	82
0.80	170	72
0.70	166	77
0.18	177	62
0.14	168	74
0.07	Very brittle	
PMMA	151	100
Polycarbonate	226	0

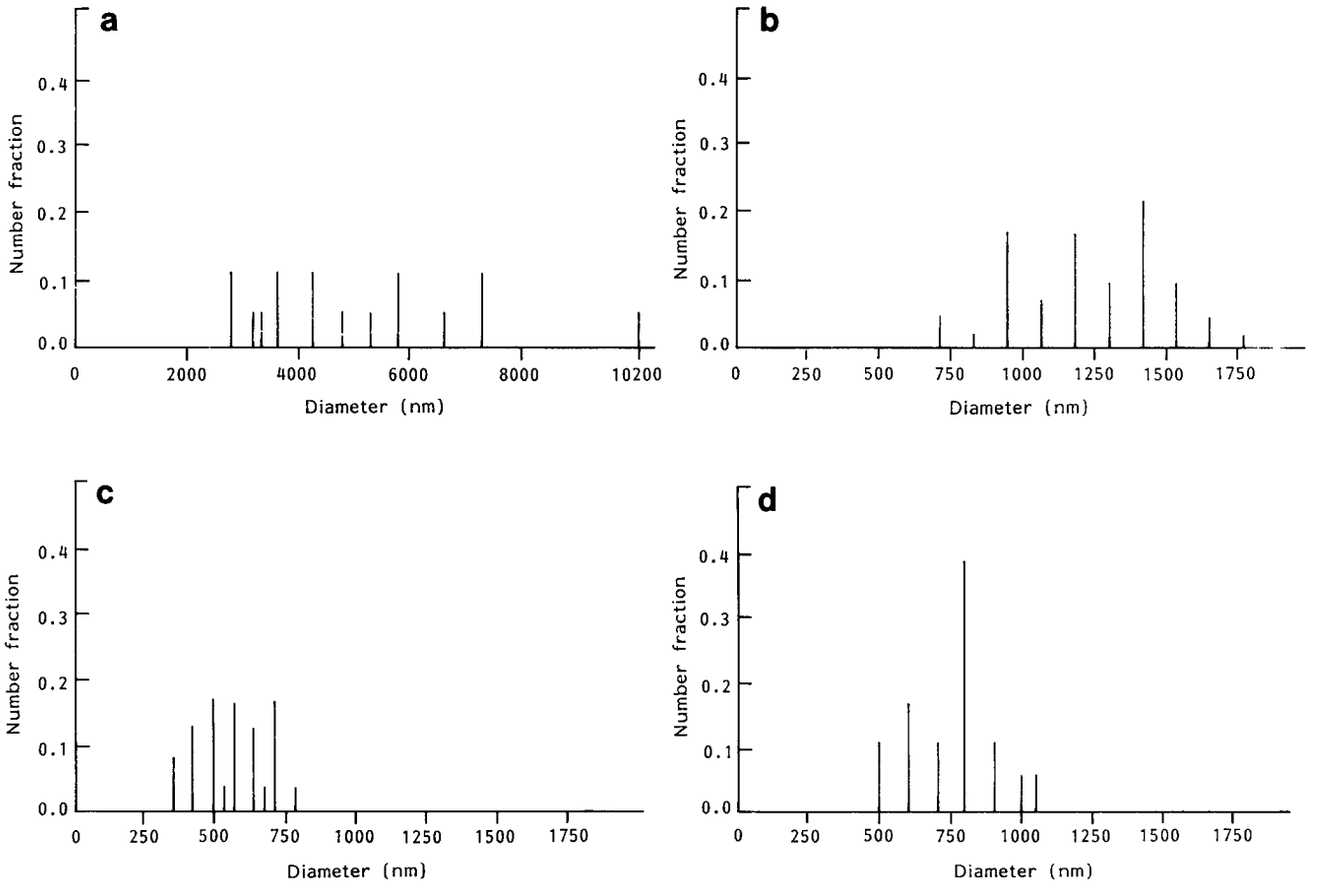

Figure 3 Histograms of the domain sizes of the polycarbonate-rich dispersions for increasing polycarbonate homopolymer molecular weight: (a) B1; (b) A4; (c) A2; (d) A3

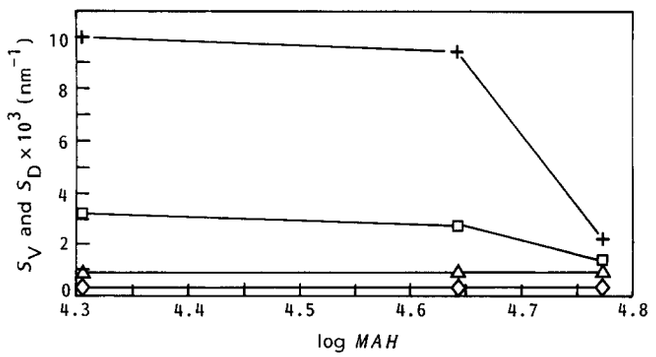

Figure 4 Variation of the interfacial area per unit volume of dispersed phase (S_D) and per unit system volume (S_V) with log *MAH*: (◇) $S_{V,0}$; (△) $S_{D,0}$; (□) S_D; (+) S_V

trend. The amount of interface generated by the copolymer increased dramatically with addition of small amounts of copolymer (1–5% w/w) and subsequently levelled off to a more or less constant value. At the same time as the molecular weight of the polycarbonate homopolymer in the blend increased from 20.2 to 72.4 kg mol^{-1}, the ability of the same copolymer to generate interface deteriorated considerably. It is interesting to note that in the system with the higher molecular weight polycarbonate an internal structure was observed in some dispersions. This, we believe, arises from the presence of copolymer chains in the dispersed phase in the early stages of phase separation which was subsequently trapped in that phase but segregated further locally when solvent was removed.

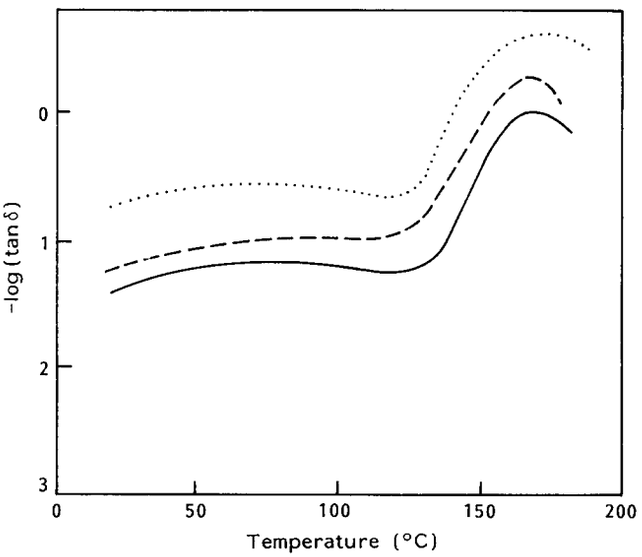

Figure 5 Logarithmic decrement peaks for systems with increasing relative polycarbonate molecular weight (*MAH/MAC*): (−) 0.14; (− −) 0.41; (··) 1.0

Phase diagrams

Figures 10 and *11* show the effects of copolymer concentration on the binodal for the quaternary systems with increasing polycarbonate homopolymer molecular weight; the extremities of the ternary diagrams represent total contents of polycarbonate and PMMA including that in the homopolymer and copolymer. They present the two extreme cases of our study with the molecular

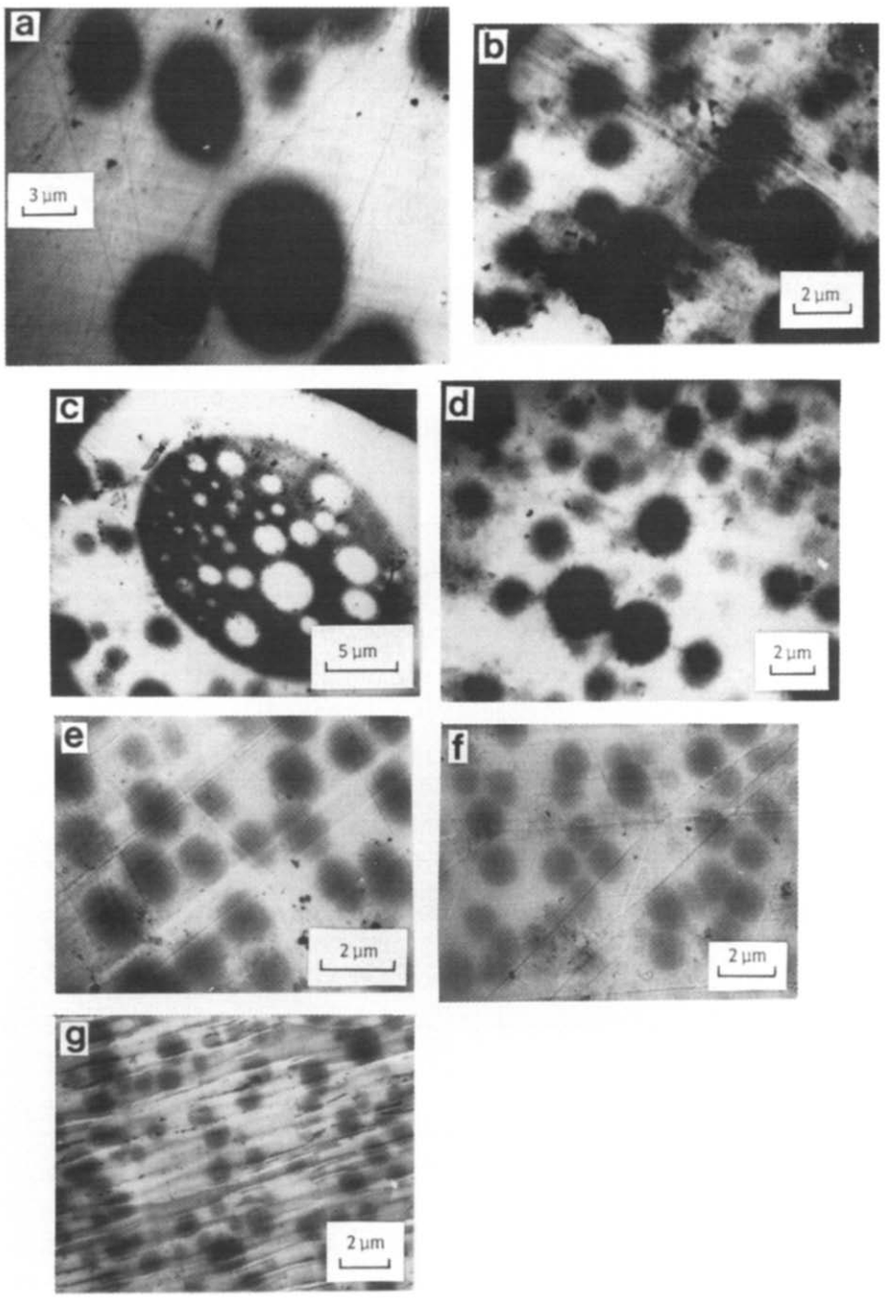

Figure 6 Effect of added copolymer concentration on morphology for system B2 (see *Table 1*): (a) 0%; (b) 1%; (c) 5%; (d) 5%; (e) 10%; (f) 30%; (g) 40%

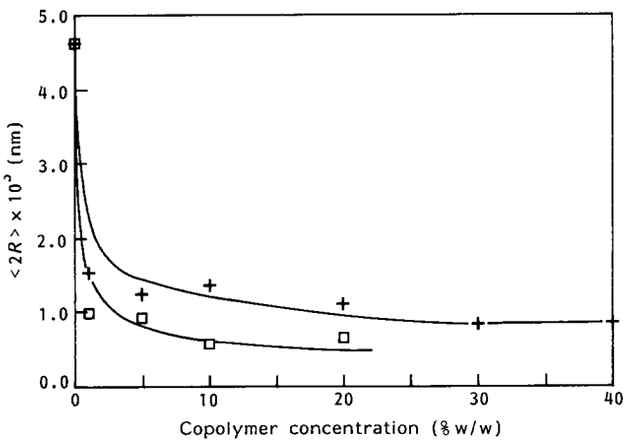

weight of the polycarbonate homopolymer being well below (*Figure 10*) and equal to (*Figure 11*) that of the corresponding copolymer block. It is interesting to note that the plait point shifted to higher total polymer concentration for the system in which polycarbonate homopolymer and block molecular weights were comparable. This effect reflects changes in the overall compatibility of the system linked with the activity of the copolymer. As the interfacial activity of the copolymer deteriorates, the presence of large copolymer molecules

Figure 7 Comparison of the efficacy of the copolymer in reducing the diameter of the polycarbonate-rich domains with increasing copolymer concentration for systems B1 and B2 (see *Table 1*). *MAH* (kg mol^{-1}): (□) 20.2; (+) 72.4

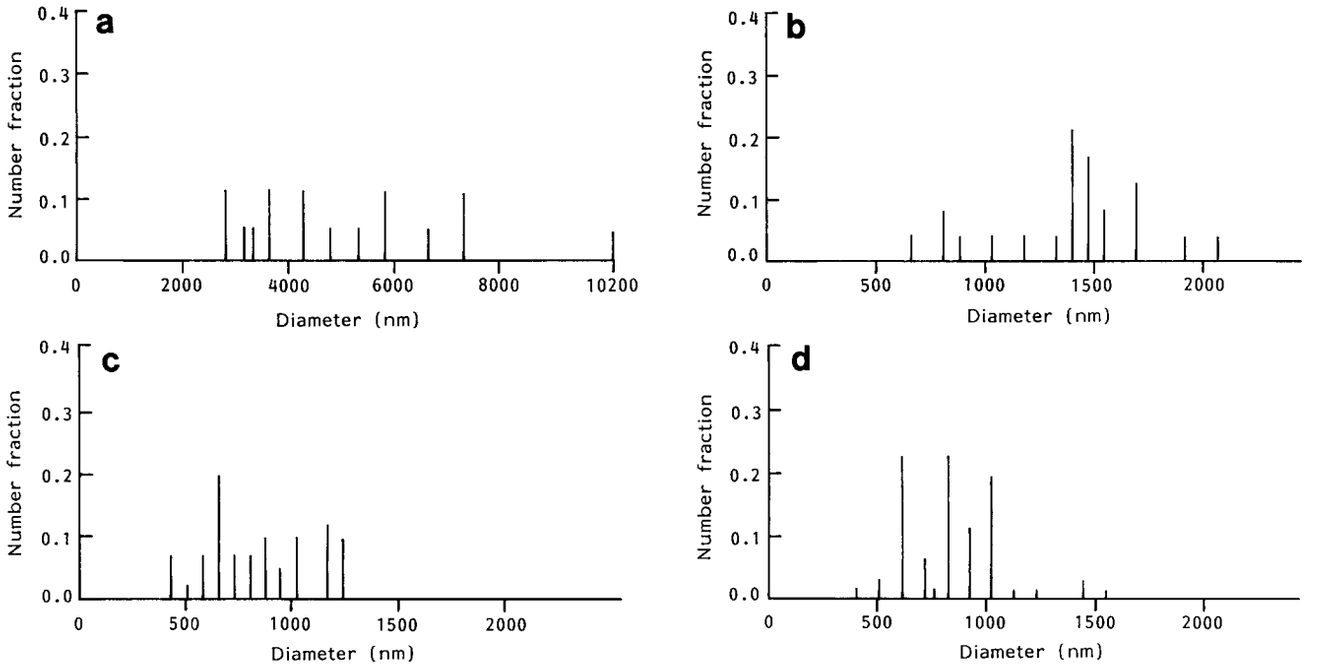

Figure 8 Histograms of the distribution of sizes of the polycarbonate-rich dispersions for system B2: (a) 0%; (b) 10%; (c) 30%; (d) 40%

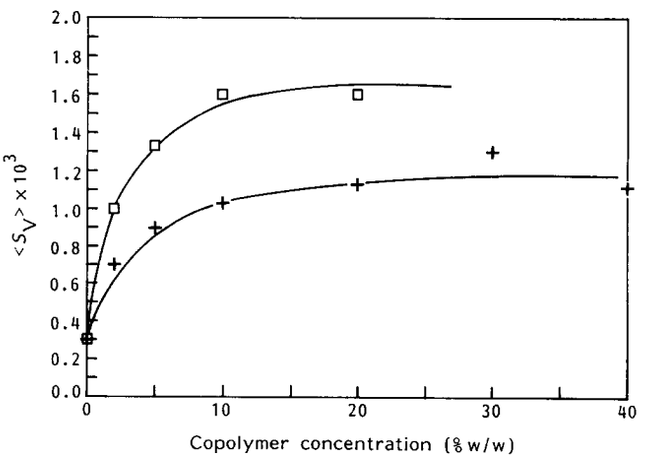

Figure 9 Comparison of the amount of interface normalized for the total system volume ($\langle S_V \rangle$) generated by the copolymer in systems B1 and B2. *MAH* (kg mol^{-1}): (□) 20.2; (+) 72.4

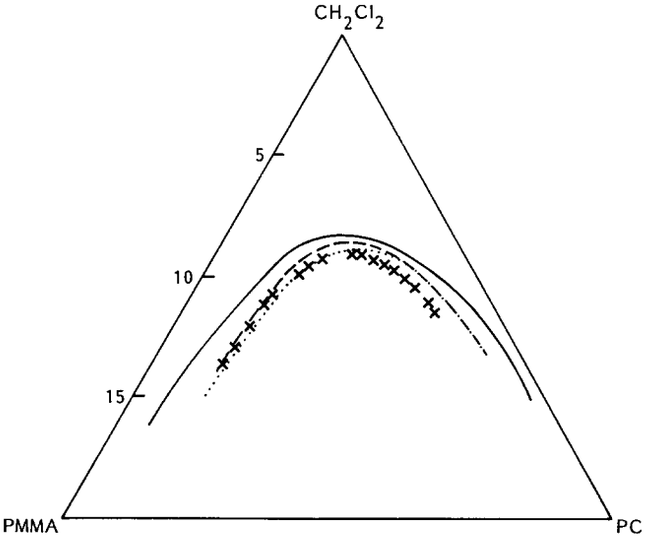

Figure 10 Phase diagram of polycarbonate (PC)/PMMA/dichloromethane (CH_2Cl_2) blends with $MAH/MAC < 1$, with varying copolymer concentration: $MAH = 20.2\,kg\,mol^{-1}$; $MAC = 143.8\,kg\,mol^{-1}$; $MBH = 48\,kg\,mol^{-1}$; $MBC = 389\,kg\,mol^{-1}$

contributes to an increased incompatibility at higher dilutions. Certainly, in both cases the systems remained incompatible in line with our previous observations that copolymers do not act as miscibilizers but as interfacial agents[7,8]. However, in both cases the presence of copolymer introduced some limited mixing as indicated by the slight inward shift of the binodal at higher concentrations of each polymer. It must be emphasized that the binodals of *Figures 10* and *11* describe the coexistence curve for the overall system. Ternary representation of quaternary systems is unable to resolve the presence of copolymer within the bulk phases, at the interface or in micellar form.

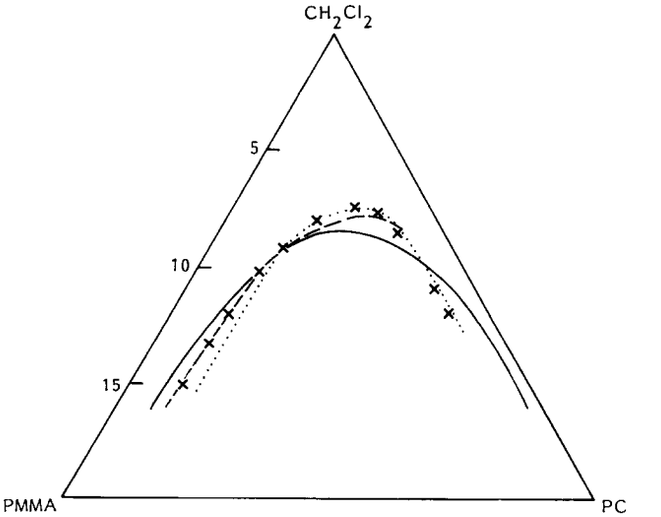

Figure 11 Phase diagram of polycarbonate (PC)/PMMA/dichloromethane (CH_2Cl_2) blends with $MAH/MAC = 1$, with varying copolymer concentration: $MAH = 20.2\,kg\,mol^{-1}$; $MAC = 20.2\,kg\,mol^{-1}$; $MBH = 48\,kg\,mol^{-1}$; $MBC = 389\,kg\,mol^{-1}$

Association of graft copolymers in toluene

The formation and characteristics of copolymer micelles are of great importance in the interpretation of the interfacial activity of copolymers in polymer blends. For this reason, the formation of copolymer micelles in toluene solutions was studied. Toluene is a selective solvent for PMMA.

Price *et al.* and others[15–18] have studied the micellization of block copolymers in selective solvents using osmometry and TEM. We have used the same techniques to investigate the behaviour of graft copolymers. *Figure 12* shows the variation of reduced osmotic pressure with copolymer concentration. The copolymer solution exhibited a marked drop in reduced osmotic pressure over a narrow concentration range and at low copolymer concentrations. This was followed by a levelling off to an approximately constant value at higher concentrations. The concentration at which the reduced osmotic pressure decreased sharply was taken as the *CMC*. The *CMC* increased with increasing temperature in agreement with observations made with poly(styrene-*b*-ethylene-*b*-propylene) triblock copolymers[17].

Micelles formed from solutions with initial concentrations (10^{-4} g cm^{-3}) below the *CMC* (10^{-3} g cm^{-3}) are shown in the TEM micrograph of *Figure 13*. The micelles were characterized by a dark core (diameter = 20 nm) surrounded by a distinctly less dark fringe (outer diameter = 63–85 nm). The interface between the core and the fringe was sharp. This picture complies with the expected morphology. Toluene is a poor solvent for polycarbonate which, therefore, forms the core of the micelle and appears dark.

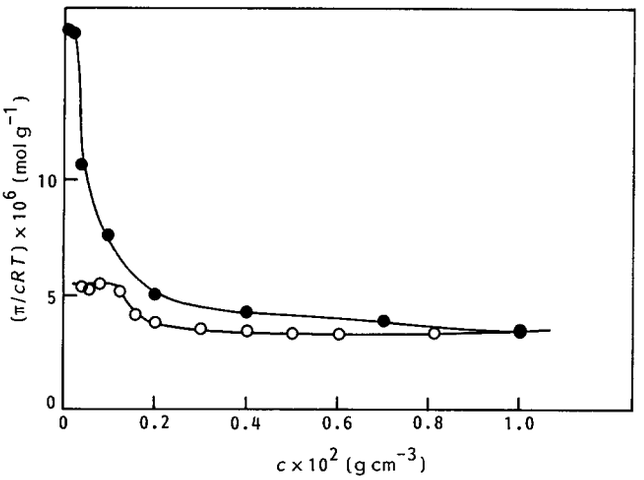

Figure 12 Variation of the reduced osmotic pressure at 310 K (●) and 321 K (○) for polycarbonate/PMMA copolymer: MAH = 143.8 kg mol^{-1}; MBC = 410 kg mol^{-1}

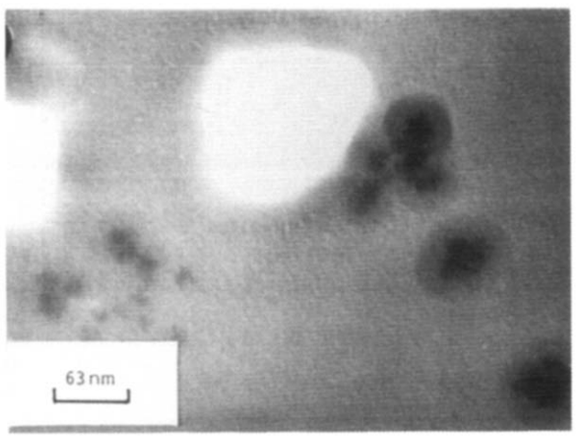

Figure 13 Transmission electron micrograph of polycarbonate/PMMA copolymer micelles on carbon grid

Table 3 Number average molecular weight of free ($\bar{M}_{n,fc}$) and associated ($\bar{M}_{n,ac}$) copolymer species determined by osmotic pressure measurements in toluene

Temperature (°C)	$\bar{M}_{n,fc}$ (kg mol^{-1})	$\bar{M}_{n,ac}$ (kg mol^{-1})
310	61.4	208.3
321	181.8	312.5

Assuming spherical geometry of the micelles, Leibler and Pincus[5] showed that the incompressibility conditions lead to the following equation:

$$(4\pi/3)R_B^3 d_B = pN_B \qquad (3)$$

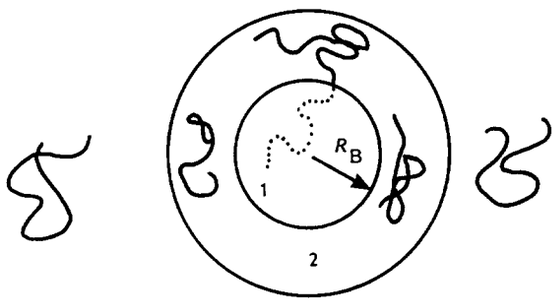

where R_B is the radius of the micelle core, N_B is the number of monomer units per chain of polycarbonate, p is the aggregation number and d_B is the density of B segments. The latter parameter can be taken as the inverse cube of the monomer length, a. Using bisphenol A as the segment of the polycarbonate chain a was approximated by a value of 10 Å. Equation (3) then gives an aggregation number of 9. Bearing in mind the complicated structure of the copolymer species and the presence of unreacted polycarbonate homopolymer, this figure must be an overestimate for the copolymer aggregation number.

The osmotic pressure data allow calculation of the number-average molar mass of the copolymer species, in the presence of unreacted polycarbonate homopolymer, in the free and associated states (*Table 3*). The $\bar{M}_n$ ratio of the free to unassociated copolymer chains (0.3) compares reasonably well to the diameter ratio obtained by TEM (0.27). However, the values calculated from the osmotic pressure were half those obtained by g.p.c. This discrepancy can only partly be attributed to the relative nature of the g.p.c. technique. The data seem to indicate that unreacted polycarbonate homopolymer did not dissolve to any great extent in the copolymer micelles under the experimental conditions used for the osmotic pressure measurements. Therefore the molecular weight determined from these experiments will be the number average of the copolymer and unreacted polycarbonate chains. The temperature dependence of $\bar{M}_n$ would further corroborate this interpretation.

Micelles in solution are in equilibrium with free chains:

$$n\mathrm{S1} \overset{k}{\rightleftharpoons} \mathrm{S}_n \qquad (4)$$

Table 4 Thermodynamic parameters for micelle formation of graft copolymers in toluene. Literature values for triblock copolymers[17] are included for comparison

Copolymer	T(K)	$CMC \times 10^{-2}$ (g cm^{-3})	$\Delta G^{\ominus}_{mic}$ (kJ mol^{-1})	$\Delta H^{\ominus}_{mic}$ (kJ mol^{-1})	$-T\Delta S^{\ominus}$ (kJ mol^{-1})
Cl	310	0.02	−38	−109	71
Cl	321	0.09	−35	−109	73
PStEP[a]	248	–	−42	−130	88

[a] Poly(styrene-*b*-ethylene-*b*-propylene)

where k is the equilibrium constant and n is the degree of aggregation.

The standard free energy change per mole of copolymer on micellization[17] can be calculated approximately from:

$$\Delta G^{\ominus} = RT \ln(CMC) \quad (5)$$

Using Van't Hoff's equation and assuming that the aggregation number and the standard enthalpy change during association are independent of temperature, Price *et al.*[17] calculated the CMC:

$$\ln(CMC) = (\Delta H^{\ominus}/RT) + \text{constant} \quad (6)$$

The standard entropy change during micellization was calculated from the difference ($\Delta G^{\ominus} - \Delta H^{\ominus}$) determined from equations (5) and (6). This calculation can only serve as a rough approximation because of the very limited number of experimental points of the function $[\ln(CMC)]/T$. It would, nevertheless, allow comparison of the sign and order of magnitude of $\Delta H^{\ominus}$ and $\Delta S^{\ominus}$ of our copolymer species to those reported for monodisperse triblock copolymers. *Table 4* summarizes the calculated thermodynamic parameters of micellization for polycarbonate/PMMA graft copolymers in toluene and compares them with those for triblock copolymers. The values calculated for the graft copolymer were comparable with those reported for the triblock copolymer of poly(styrene-*b*-ethylene-*b*-propylene)[17]. In agreement with earlier observations, the enthalpy contribution to the free energy change is solely responsible for micelle formation. The entropy contribution is unfavourable for micelle formation. This behaviour is the opposite of that of anionic surfactants in aqueous systems.

GENERAL DISCUSSION

The average area occupied by a single copolymer molecule at the interface in a blend (α) and the average area per copolymer junction can provide information about the efficiency of the copolymers in generating interface and stabilizing the polycarbonate-rich domains against coalescence. The former can be calculated from a simple equation derived by Paul[1]:

$$\alpha = 3\Phi_A M/\langle R\rangle N_A W d \quad (7)$$

where M is the total molecular weight taken as $M = MAC + MBC$, W is the weight fraction, $\langle R\rangle$ is the average radius of the polycarbonate-rich dispersions, Φ_A is the volume fraction of the polycarbonate in the blend and N_A is Avogadro's number. The density (d) was assumed to be 1 g cm^{-3}. Equation (7) assumes that *all* copolymer molecules are located at the interface. *Figure 14* compares the average area per copolymer molecule for systems with polycarbonate chains with molecular weights of 20.2 and 72.4 kg mol^{-1}. No major differences in the average interfacial area per copolymer were observed between the two systems. In both cases the copolymers acted as very efficient interfacial agents at low copolymer contents (< 10% w/w). Large amounts of interface and fine dispersions were created by very little copolymer. The area occupied by a single copolymer molecule at the interface decreased rapidly at low copolymer contents. Our calculations show that copolymer molecules occupy an average area of 10–100 nm^2 at the interface. This area can be compared with estimated values of the root-mean-square radius of gyration of our graft copolymers ($\langle s^2\rangle^{1/2}$) using equation (8):

$$\langle s^2\rangle = gCnl^2/6 \quad (8)$$

where C is a constant characteristic of the chain structure, l is the bond length and n is the number of bonds[20]. Parameter g accounts for the non-linearity of our species and does not exceed a value of 0.7 reported for random branching by Zimm and Stockmayer[21]. Assuming the molecular weight of our copolymers is given by ($MAC + MBC$) the area occupied by a single copolymer molecule calculated from the molecular dimensions is 2.3–2.7 nm^2. Comparison of these figures with those calculated from the electron micrographs suggests that the interface is dilute in copolymer at low copolymer concentrations in the blend (< 10%). This is consistent with creation of large amounts of interface by a few per cent of added copolymer. Although the interfacial area occupied by a single copolymer molecule reduced slowly

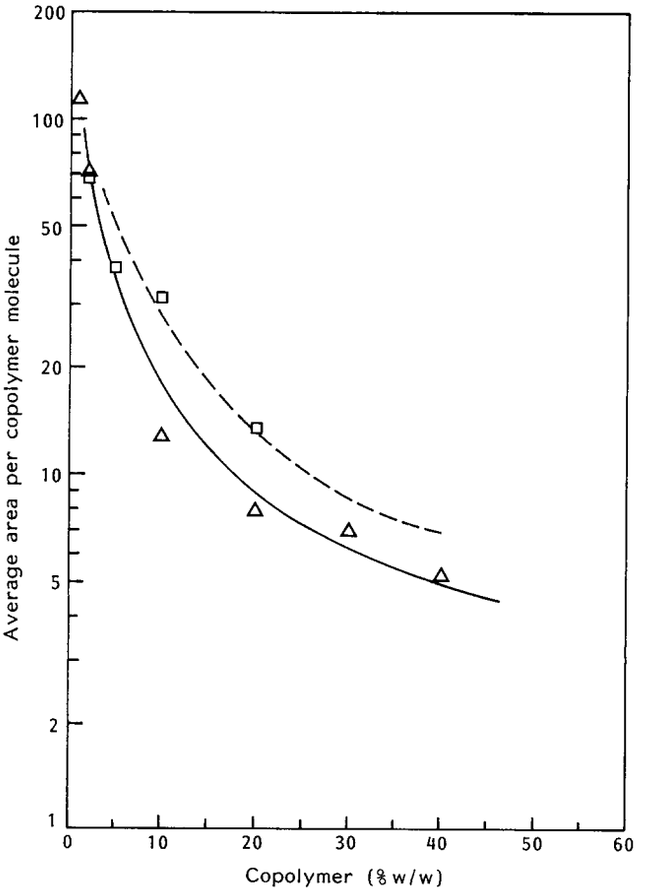

Figure 14 Variation of the average area occupied by a single copolymer molecule at the interface in systems containing polycarbonate homopolymer of 20.2 (□) and 72.4 (△) kg mol^{-1}

on further addition of copolymer into the system, the size of the polycarbonate-rich dispersions remained almost constant up to 20% w/w copolymer. We believe that the additional copolymer will find it increasingly energetically difficult to create a new interface. It will either be incorporated in the bulk phase or form a separate phase[8]. The latter will take the form of copolymer micelles or microdomains of size below the detection limits of our microscopy technique. This is consistent with the presence of a single broad $\tan\delta$ relaxation in the dynamic mechanical spectra. In the limit of 100% copolymer, the copolymer blocks will microphase separate. In this case the interfacial area per single copolymer molecule will correspond to that calculated from the molecular dimensions according to equation (8). Copolymer molecules in the blend with the longer polycarbonate homopolymer chains occupied slightly smaller interfacial area (*Figure 13*). This reflects the smaller amount of interface available in the system as shown in *Figure 8*.

The increase in the diameter of the polycarbonate-rich domains with increasing molecular weight of polycarbonate homopolymer can, in the first instance, be accounted for by swelling of the domains with increasingly longer chains. This can only provide a limited contribution since the mean-square end-to-end distance of a statistical chain ($\langle r^2\rangle^{1/2}$) is a linear function of the degree of polymerization [equation (9)][20]. It would not, therefore, explain the significant increase in the average domain diameter at higher polycarbonate homopolymer molecular weights.

$$\langle r^2\rangle = Cnl^2 \qquad (9)$$

A more comprehensive explanation involves the changes in the thermodynamics of the system with varying homopolymer molecular weight. *Figure 15* illustrates the influence of decreasing homopolymer molecular weight on the miscibility of the two homopolymers. The compatibility of the PMMA/polycarbonate/dichloromethane system increased as the molecular weight of the polycarbonate decreased, as shown by the shift of the binodal to higher total polymer concentrations. Reduced polymer demixing will lead to a less significant drop in the interfacial tension hindering the creation of a new interface in the blend. Increasing numbers of copolymer molecules will be expected, in that case, to remain in the bulk phase.

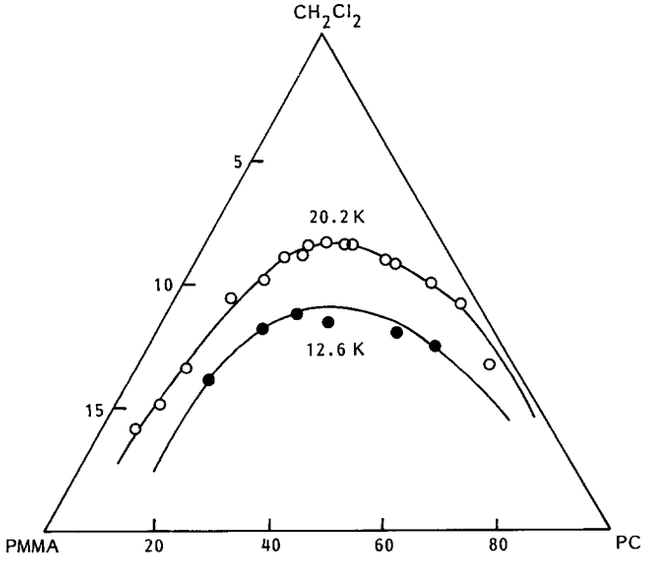

Figure 15 Phase diagram of a PMMA/polycarbonate (PC)/dichloromethane (CH_2Cl_2) ternary system with increasing polycarbonate homopolymer molecular weight

The deterioration in copolymer interfacial activity at higher polycarbonate molecular weights is closely linked to the mechanism of the whole process.

We know from the work in toluene that the graft copolymers can form micelles at very dilute solutions in selective solvents. The solvent used in this work, dichloromethane, is a non-selective solvent. No association of the copolymer molecules is therefore expected to take place until their 'environment' becomes a selective solvent. The system would remain homogeneous until it crosses the binodal. At this point the minor component(s) will form nuclei, that is aggregates of a small number of chains dispersed in a PMMA-rich matrix. The observations in phase diagrams of copolymer modified blends with $MAH/MAC<1$ have shown that the binodal does not alter dramatically as the copolymer content increased up to 13% w/w. In the opposite case, $MAH/MAC=1$, the critical point shifted to lower total polymer concentrations with addition of copolymer. Unfortunately, the ternary representation does not resolve the phase behaviour of all the species of the quaternary system. Let us consider for the sake of argument that the polycarbonate homopolymer is rejected from the PMMA-rich matrix when the system crosses the binodal (*Figure 15*). We shall now consider the possible mechanisms, involving the copolymers, that can lead to fine polycarbonate-rich dispersions stable against coalescence by the copolymer chains in the case $MAH/MAC<1$. The copolymer molecules will have three options at that point:

I. They will form a separate phase dispersed in the PMMA-rich matrix. This will possibly involve formation of micelles similar, in principle, to those observed in toluene. They will consist of a polycarbonate core surrounded by a PMMA fringe.
II. They will remain dispersed on a molecular level within the PMMA-rich matrix and they will subsequently adsorb onto the surface of the growing polycarbonate-rich domains.
III. The copolymer molecules will be involved in the phase separation of the quaternary system.

Formation of copolymer micelles (option I) would not account for the presence of the fine polycarbonate-rich domains (400–500 nm in diameter) with addition of copolymer. The TEM data on copolymer segregation in selective solvents showed micelles with a core diameter of 20 nm. The final morphology would therefore require swelling of this micelle core by at least 20 times its original volume. In this case the polycarbonate homopolymer chains will have to diffuse from the PMMA-rich matrix and/or the polycarbonate-rich domains into the core of the copolymer micelles. There is no reason for the polycarbonate homopolymer to dissolve preferentially into the copolymer micelle core rather than the polycarbonate homopolymer-rich domains. The osmotic pressure measurements suggest that the micelles will not be swelled by polycarbonate homopolymer of molecular weight equal to that of the copolymer block to any

considerable extent. This is corroborated by a considerable body of experimental evidence[22–24]. The polycarbonate homopolymer will, under these conditions, tend to segregate into separate phases which will not be stabilized against coalescence during solvent evaporation.

The second option will account for the stability of the growing polycarbonate-rich domains against coalescence during film formation, in agreement with the fine polycarbonate-rich dispersion observed on addition of copolymer to the blend. This process cannot however explain the significance of the relative molecular weight *MAH/MAC* to the interfacial activity of the copolymer. From experiments with both polymeric and other organic systems, it is well documented that physical adsorption is not dependent on this parameter[25,26].

In the third option, the final morphology will involve participation of the copolymer molecules in the phase separation processes as the system crosses the binodal. This leads potentially to the formation of copolymer–homopolymer nuclei which will be involved subsequently with phase rearrangement to give rise to polycarbonate-rich domains. These growing polycarbonate-rich domains will be sterically stabilized against coalescence during film formation, as in option II. More importantly, this mechanism will account for the importance of the relative molecular weight of the copolymer block to that of the corresponding homopolymer. The relative molecular weight of the polycarbonate homopolymer to that of the copolymer block will control the nature of the onset of phase separation. This is in agreement with the logarithmic dependence of the amount of homopolymer which can be solubilized within the corresponding copolymer block on the relative molecular weight of this component calculated by Meier[27]. The problem can, at this stage, be reduced to the effect of *MAH* and *MAC* on the compatibility of polycarbonate homopolymer with the polycarbonate block.

The importance of *MAH/MAC* can be demonstrated by means of a simple mean field treatment[20] reported by Inoue *et al.*[28]. The free energy of mixing, ΔG_m, for the copolymer AB/homopolymer A/solvent (S) ternary system is given by:

$$\Delta G_m = kT[n_C \ln \Phi_C + n_H \ln \Phi_H + \chi n_C(\Phi_A - \sigma_A)] \quad (10)$$

where subscripts C and H denote the copolymer and homopolymer. The copolymer composition is given by the mole fraction of A in the copolymer:

$$\sigma_A = x_A/(x_A + x_B) \quad (11)$$

where x denotes the degree of polymerization.

The enthalpic part of the interaction between the homopolymer and copolymer is described by the χ parameter:

$$\chi = z\Delta W_{AB} x_A/kT \quad (12)$$

where z is the lattice co-ordination number taking values of 8 for the cubic and 12 for the hexagonal lattice, and ΔW_{AB} is the difference in the contact energy between units A and B.

The critical total polymer concentration for phase separation (c^*) can be determined in the conventional way:

$$c^* = (1 + r^{-1/2})^2/2\sigma_A \quad (13)$$

where r is the ratio of the degree of polymerization of the homopolymer to that of the copolymer:

$$r = x_H/x_C \quad (14)$$

This is obviously a function of β, $\beta = x_{AH}/x_{AC}$:

$$r^{-1} = \beta^{-1} + x_{BC}/x_{AH} \quad (15)$$

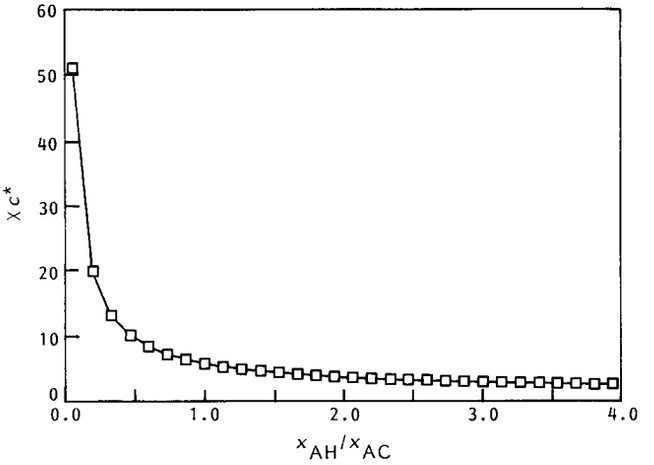

Figure 16 χc^* values as a function of x_{AH}/x_{AC} according to equation (12)

Figure 16 illustrates the variation of χc^* with increasing β calculated for a ternary system with $x_{BC} = 1500$, $x_{AC} = 4500$ and x_{BH} varying from 1000 to 60 000. The numerical calculation is qualitative rather than quantitative. It is interesting to note that as β increases towards 1, χc^* decreases dramatically. The critical point appears to be located at around $\beta = 0.5$. A significant change in χc^* is still observed for $0.5 \leqslant \beta \leqslant 1.0$. At values of > 1, the decay of χc^* with increasing β has slowed down noticeably.

We believe that the relative position of the critical concentration for the copolymer/homopolymer system, corresponding to the minor phase, with respect to the plait point for the homopolymer/homopolymer blend controls the contribution of *MAH/MAC* to the final film morphology. As the molecular weight of the polycarbonate homopolymer is reduced, c^* increases dramatically. This means that the polycarbonate homopolymer remains compatible with the polycarbonate block to higher total polymer concentrations. This allows full utilization of option III leading to a large number of fine polycarbonate-rich dispersions. On the other hand, as the molecular weight of the homopolymer approaches that of the polycarbonate block, c^* shifts to more dilute solutions. This leads to a mechanism described increasingly by options I and II. The polycarbonate homopolymer will not be compatible with the corresponding block and will not co-participate in the initial phase separation process. This leads to the formation of separate phases limiting the potential of the copolymer to stabilize the polycarbonate-rich domains. Some copolymer chains will potentially absorb on the growing polycarbonate-rich phases at random. This can generate a whole population of polycarbonate-rich domains in the final film morphology. The experimental evidence suggests that either this process is not efficient in stabilizing the polycarbonate-rich domains or that it does not happen to any significant extent[29].

An approximate phase diagram for the quaternary system can now be constructed from the experimental data and critical concentration calculations. The basic

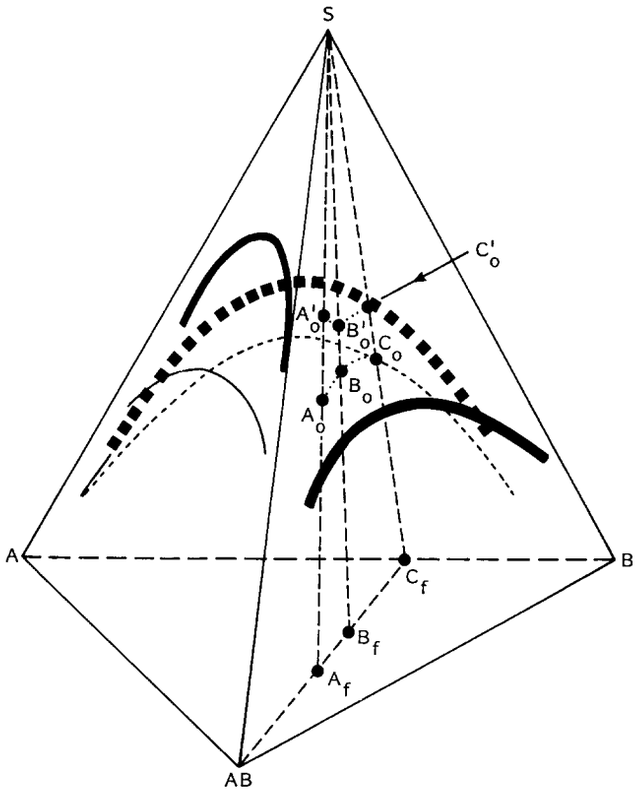

Figure 17 Complete phase diagram for the quaternary system dichloromethane (S)/PMMA (B)/polycarbonate (A): bold lines correspond to systems with *MAH/MAC* close to 1; narrow lines correspond to systems with *MAH/MAC* well below 1; broken lines are off the plane

characteristics of this phase diagram are illustrated by *Figure 17*. In the case $MAH/MAC<1$, the system is dissolved in a non-selective solvent and the binodal surface is relatively 'even'. This is in agreement with the unaltered position of the plait point of *Figure 10* with increasing copolymer concentration. As the molecular weight of the polycarbonate homopolymer increases the critical concentration for the copolymer/polycarbonate/dichloromethane system and the plait point for the polycarbonate/PMMA/dichloromethane system shift to higher dilutions as shown by experiment and calculation. This produces a binodal surface skewed towards the planes (S, A, B) and (S, A, AB). This is also in agreement with the observed shift in the plait point in the ternary representation of *Figure 11*. Lines $C_0B_0A_0$ and $C'_0B'_0A'_0$ are the loci of plait points with increasing copolymer content in the case of $MAH<MAC$ and $MAH=MAC$, respectively. Lines SC_f, SB_f and SA_f are the isopleths followed by the system with increasing copolymer content. This phase diagram describes the phase changes during solvent evaporation as the polycarbonate homopolymer molecular weight increases at constant copolymer content. Two processes predominate the phase behaviour of the system as it crosses the binodal surface: phase separation in the copolymer/homopolymer pair and homopolymer demixing. The relative position of those two binodals dictates the efficiency of the copolymer to generate fine stable dispersions. In the case $MAH/MAC<1$, the system will begin phase separation at B_0 through concurrent nucleation and growth of all the three polymeric species with PMMA forming the matrix. In the limiting case $MAH/MAC=1$, the system will cross the binodal surface at B'_0, that is at higher dilutions. The critical point calculations have shown an abrupt increase in c^* as MAH/MAC exceeds a certain value (~ 0.5). This will induce A/AB type phase separation well before A/B and AB/B. Homopolymer A will therefore be rejected from the stabilizing species eliminating the possibility for formation of stabilized A-rich domains.

It is interesting to note that a requirement for the mechanism based on option III is that the interface is dilute in copolymer so as to facilitate easy diffusion of polycarbonate homopolymer chains from the matrix to the polycarbonate-rich phases during the growth process. This is in agreement with our TEM data.

ACKOWLEDGEMENTS

We would like to thank Mrs Ann Leyden for the skilful preparation of the polycarbonate prepolymers. The authors would like to thank ICI for supporting this programme under the Joint Research Scheme which provided a Postdoctoral Fellowship for one of us (PS).

REFERENCES

1 Paul, D. R. in 'Polymer Blends' (Eds D. R. Paul and S. Newman), Vol. 2., Academic Press, New York, 1978, p. 35
2 Riess, G., Kohler, J. and Banderet, A. *Makromol. Chem.* 1967, **101**, 58
3 Gaillard, P., Ossenbach-Sauter, M. and Riess, G. *Makromol. Chem., Rapid Commun.* 1980, **1**, 771
4 Leibler, L., Orland, H. and Wheeler, J. C. *J. Chem. Phys.* 1983, **79**(7), 3550
5 Leibler, L. and Pincus, P. *Macromolecules* 1984, **17**, 2922
6 Noolandi, J. and Hong, K. M. *Macromolecules* 1987, **15**, 482
7 Eastmond, G. C., Ming, J. M. and Malinconico, M. *Br. Polym. J.* 1987, **19**, 275
8 Sakellariou, P., Eastmond, G. C. and Miles, I. S. *Polymer* 1991, **32**, 2351
9 Phillips, D. G. *PhD Thesis* University of Liverpool, 1976
10 Bamford, C. H., Dyson, R. W. and Eastmond, G. C. *J. Polym. Sci. C* 1987, **16**, 2425
11 Bamford, C. H., Dyson, R. W. and Eastmond, G. C. *Polymer* 1969, **10**, 885
12 Bamford, C. H. and Eastmond, G. C. in 'Recent Advances in Polymer Blend, Grafts and Blocks' (Ed. L. H. Sperling), Plenum Press, New York, 1974, p. 1645
13 Bamford, C. H., Eastmond, G. C. and Whittle, D. *Polymer* 1969, **10**, 771; Eastmond, G. C. and Richardson, J. E. *Macromolecules* 1991, **24**, 3189
14 Eastmond, G. C. and Harvey, L. W. *Br. Polym. J.* 1985, **17**, 975
15 Booth, C., Naylor, T., Price, C., Rajab, N. S. and Stubbersfield, R. B. *J. Chem. Soc., Faraday Trans. 1* 1978, **74**, 2352
16 Price, C., Chan, E. K. M., Hudd, A. L. and Stubbersfield, R. B. *Polym. Commun.* 1986, **27**, 196
17 Price, C., Kendall, K. D., Stubbersfield, R. B. and Wright, B. *Polym. Commun.* 1983, **24**, 326
18 Price, C., McAdam, J. D. G., Lally, T. P. and Woods, D. *Polymer* 1974, **15**, 228
19 Danon, J. *Eur. Polym. J.* 1970, **6**, 299
20 Flory, P. 'Principles of Polymer Chemistry', Cornell University Press, Ithaca, 1978
21 Zimm, B. H. and Stockmayer. W. H. *J. Chem. Phys.* 1949, **17**, 1301
22 Tuzar, Z. and Kratochvil, P. *Makromol. Chem.* 1973, **170**, 177
23 Skoulios, A., Hoeffer, P., Gallot, Y. and Selb, J. *Makromol. Chem.* 1970, **148**, 305
24 Roe, R.-J. Technical Report No. 11, Office of Naval Research, 1984
25 Santore, M. M., Russel, W. and Prud'homme, R. K. *Macromolecules* 1989, **22**, 1317
26 Cosgrove, T. and Vincent, B. in 'Fluid Interfacial Phenomena' (Ed. C. A. Croxton), J. Wiley and Sons, Chichester, 1986, Ch. 7
27 Meier, D. *Am. Chem. Soc. Div. Polym. Chem. Polym. Prepr.* 1970, **11**, 400
28 Inoue, T., Soen, T., Hashimoto, T. and Kawai, H. *Macromolecules* 1970, **3**, 87
29 Sakellariou, P., Eastmond, G. C. and Miles, I. S. unpublished results